www.papersinphysics.org

Received: 11 October 2024, Accepted: 01 August 2025
Edited by: D. Zanette, Bariloche Atomic Centre, Argentina
Licence: Creative Commons Attribution 4.0
DOI: https://doi.org/10.4279/PIP.170004

ISSN 1852-4249

Wavelet q-extropies of fractal signals

Julio César Ramírez Pacheco[1*], Joel Antonio Trejo Sánchez[2†], Luis Rizo Domínguez[3‡]

The standard Tsallis and Rényi extropies of parameter q are extended to the time-scale domain, and closed-form expressions of these extropies for fractal signals of parameter α are obtained. Wavelet extropy planes are computed for a range of the fractality parameter α and signal length N which allows an unveiling of the properties and potential applications of wavelet q-extropies on fractals. Results indicate that wavelet q-extropies allow accurate description of the complexities of fractals since they are maximum for completely random samples, decreasing for correlated fractals and increasing for uncorrelated fractals. Unlike Shannon and Rényi, Tsallis extropies display a constant region, symmetric on α, which allows classification of fractals based on a simple heuristic of wavelet extropy values. Finally, the application of wavelet Tsallis extropies allows the differentiation of electroencephalogram (EEG) times series from volunteers with eyes closed and eyes open.

I Introduction

Information theory quantifiers such as Shannon, Tsallis and Rényi entropies are employed in the literature to quantify the complexity and information content of a variety of real world data. For instance, Tsallis entropies have been used to study the complexities associated with electroencephalogram (EEG) signals [1], structural damage identification [2] and for analizing event-related potentials in neuroelectrical signals [3, 4], to name but a few. Although entropies are usually computed using the raw measured signals (time-domain) they can also be computed in other representations of the signal such as their Fourier domain (spectral entropies) and their time-scale domain (wavelet entropies). Wavelet entropy [5–7], wavelet (q, q')-entropies [8] and wavelet Fisher's informations [9, 10] have made the application of information-theory quantifiers more widespread in the literature. Wavelet Tsallis entropies, e.g., have been used for general stochastic processes [11], fractal signal classification [12], detection of level-shifts in fractal time series [13] and for the characterization of energy prices [14]. Further information theory quantifiers include, but are not limited to, Fisher-Shannon information planes [15], LMC complexity [16] and the more recent Fractal Belief Rényi (FBR) divergence [17] and higher order fractal belief Rényi divergence (HOFBeRD)[18], employed in pattern classification to measure discrepancy and expected to be applied in the complexity analysis of electroencephalogram data to detect migraine and depression. In addition, Quantum X-entropy [19] is being proposed to measure uncertainty and is expected to make a profound contribution in biological signal analysis. Recently, the extropy concept has been proposed in the literature. Extropy, according to Lad and co-workers [20], is a complementary dual of information entropy and may provide valuable and complementary information about the complexity of a signal. Tsallis, Rényi and Ginni extropies have been studied in [21–23] along with some

* juliocr@uqroo.edu.mx
† joel.trejo@cimat.mx
‡ lrizo@iteso.mx

1 División de Ciencias Multidisciplinarias Cancún, Universidad Autónoma del Estado de Quintana Roo, SM 260, Mza 21 ý 16, Lt 1-01, Fraccionamiento Prado Norte, Cancún, Quintana Roo, México.

2 SECIHTI- Centro de Investigación en Matemáticas.

3 Departamento de Electrónica, Sistemas e Informática, ITESO.

applications to some theoretical probability functions. Extropies are a recent development and are currently considered as a research hotspot in statistics. In this contribution, wavelet Rényi and Tsallis q-extropies of fractal signals are obtained, and, likewise, wavelet Tsallis q-entropies for these signals were computed. Moreover, extropy planes are obtained and the characteristics for fractal signals studied in some detail. Furthermore, based on these planes, it is possible to claim which information extropy is more suitable for the analysis of fractals and highlight potential applications. The rest of the paper is structured as follows: Section II briefly overviews the concept of wavelets and the wavelet analysis of fractal signals of parameter α. Important results on wavelet analysis of fractal signals are highlighted along with definitions that are essential for the understanding of the rest of the article. Later, Section III presents the main contributions of the article, which are the wavelet Rényi and Tsallis q-extropies of fractal signals. In addition, extropy planes are obtained for each quantifier and, based on these, a complete characterization of these extropies for fractals is presented. Furthermore, potential applications are highlighted in this section. Finally, Section IV presents the conclusions of the paper.

II Materials and methods

Extropies obtained in this contribution are based on wavelets, therefore a brief discussion of the wavelet analysis of fractals signals is presented.

i Wavelet analysis of fractals

Wavelet transforms play a special role in the analysis of signals in physics [24] and other scientific areas [25,26]. Wavelet transforms can be categorized based on the nature of the scaling and shifting procedures as continuous wavelet transforms (CWT) and discrete wavelet transforms (DWT). The DWT of a signal X_t is given by:

$$d_X(j,k) = \int_{-\infty}^{\infty} X_t\, \psi_{j,k}(t)\, dt, \quad (1)$$

where $\psi_{j,k}(t) = 2^{-j/2}\psi(2^{-j}t - k)$ is a dyadically scaled and integer-translated mother wavelet $\psi(t)$. For fractal signals, the first and second order moments of the DWT are of primary importance. The first moment is defined as follows,

$$\mathbb{E}d_X(j,k) = 2^{-j/2}\int_{-\infty}^{\infty} X(t)\psi(2^{-j}t - k)dt, \quad (2)$$

while the second, also known in the literature as the wavelet spectrum [27], takes the form

$$\mathbb{E}d_X^2(j,k) = \int_{-\infty}^{\infty} S_X(2^{-j}f)|\Psi(f)|^2\, df, \quad (3)$$

where $\Psi(f) = \int \psi(t)\mathrm{e}^{-j2\pi ft}\, dt$ is the Fourier transformation of $\psi(t)$, $S_X(.)$ is the power spectral density (PSD) of the process X_t and $\mathbb{E}$ the expectation operator. For fractals, the PSD is $S_x(f) \sim c|f|^{-\alpha}$ and thus substituting this well-known PSD into Eq. (3) results in the wavelet spectrum of fractals signals of parameter α [27], i.e.,

$$\mathbb{E}d_X^2(j,k) = C2^{j\alpha}, \quad (4)$$

where C is a constant. From equation (4), the wavelet energy at scale j can be computed as [6],

$$p_j = \frac{\mathbb{E}d_X^2(j,k)}{\sum_j \mathbb{E}d_X^2(j,k)}. \quad (5)$$

Wavelet energy p_j satisfies the axioms of probability, i.e., $0 \le p_j \le 1$, $\sum_j p_j = 1$ and is therefore a probability mass function (pmf) which represents the probability that the energy of a signal is at wavelet scale j. From the wavelet energy p_j, many statistical quantities can be computed including Shannon entropy, Tsallis extropies, Rényi extropies and other information theory quantifiers such as Fisher-Shannon information planes, among others. For fractal signals, the wavelet energy, p_j, is given by,

$$p_j = 2^{(j-1)\alpha} \times \frac{1-2^{\alpha}}{1-2^{\alpha N}}, \quad (6)$$

where α is the fractality parameter and N is the number of scales considered within a signal. For further information on wavelets, the interested reader may refer to [24, 25, 28, 29] and for the analysis and estimation of fractals refer to [30–32].

ii Information theory quantifiers

Entropy measures the information content or uncertainty of a random signal or system. Several information measures have been proposed in the literature and can be classified in a general sense as extensive or nonextensive. Shannon entropy is an extensive entropy and is appropriate for stationary signals with no correlation structure, short-range forces, and which is defined as

$$\mathcal{H}(p) = -\sum_j p_j \log(p_j), \tag{7}$$

where p_j is a pmf. Rényi entropy is also extensive but provides a parameter q which adds flexibility and the possibility of adjusting the analyses with q. It is defined as

$$\mathcal{H}_q^R(p) = \frac{\log(\sum_{j=1}^N p_j 1)}{1-q}, \tag{8}$$

where $q \neq 1$. Tsallis entropy, on the oher hand, is a nonextensive entropy and is appropriate for signals with long-range forces, long-range interactions and nonstationary signals. The Tsallis entropy of parameter q is defined as

$$\mathcal{H}_q^T(p) = \frac{1-\sum_{j=1}^N p_j^q}{q-1}. \tag{9}$$

Rényi and Tsallis entropies converge to Shannon entropy when $q \to 1$ but they are not related to each other. Extensive and non-extensive entropies can be further extended if entropies are computed in a different representation of the signal. For instance, when the entropies are computed in a wavelet-based representation of the signal by means of the wavelet spectrum, then they are called wavelet entropies. Wavelet-based information quantifiers have shown to be appropriate for the analysis of fractal signals [5,6] and several analysis frameworks based on them have been proposed.

iii Information extropies

Recently, the concept of extropy has been introduced as a complementary dual of Shannon entropy [20]. Extropy can further complement the analysis based on entropy and provide valuable information in the analysis of a phenomena. For a pmf p_j, extropy is defined as

$$\mathcal{J}(p) = -\sum_j (1-p_j)\log_2(1-p_j). \tag{10}$$

Rényi extropy is a complementary dual of Rényi entropy [22]. Rényi extropy extends the extropy concept by providing an additional parameter q which adds flexibility. Rényi extropy is defined as

$$\mathcal{J}_q^R(p) = \frac{-(N-1)\log(N-1)}{1-q} + \frac{(N-1)\log\left(\sum_{j=1}^N (1-p_j)^q\right)}{1-q}, \tag{11}$$

and when $q \to 1$, Shannon extropy results. Tsallis extropy is a complementary dual of Tsallis entropy. Tsallis extropy is defined for a pmf p_j as

$$\mathcal{J}_q^T(p) = \frac{N-1-\sum_{j=1}^N (1-p_j)^q}{q-1}. \tag{12}$$

When $q \to 1$ Shannon extropy results. Several other extropy meausures have been proposed in the literature, such as Ginni extropy [23] and belief eXtropy [33] as well as applications in pattern recognition [34] and algorithms for estimating extropy from data [35]. The main result of the present contribution is to propose wavelet q-extropies and to characterize these extropies for fractal signals of parameter α. As a matter of fact, wavelet Shannon extropy or simply wavelet extropy is obtained by direct application of Eq. (6) into Eq. (10) which results in,

$$\mathcal{J}(p) = \sum_{n=1}^{\infty} \frac{(-1)^{n-1}}{n}\left(\frac{2^\alpha - 1}{1-2^{\alpha M}}\right)^n \times \left\{\frac{1-2^\alpha}{1-2^{\alpha M}}\frac{1-2^{(\alpha+\alpha n)M}}{1-2^{(\alpha+\alpha n)}} - \frac{1-2^{\alpha n M}}{1-2^{\alpha n}}\right\}. \tag{13}$$

This expression permits characterization of complexities of fractals of parameter α. In the following, wavelet q-extropies are obtained by direct application of Eq. (6) into Eq. (11) and (12).

III Results and discussion

Wavelet Tsallis q-extropy is obtained by direct application of (4) into Eq. (12) which gives

$$\mathcal{J}_q^T(p) = \frac{1}{q-1} \times \left\{N - 1 - \sum_{k=0}^{q}\left(\frac{1-2^{\alpha k N}}{1-2^{\alpha k}}\right) \times \left(\frac{2^\alpha - 1}{1-2^{\alpha N}}\right)^k \binom{q}{k}\right\}. \tag{14}$$

From this equation, properties and applications may be identified via the so-called extropy planes, which are defined as follows:

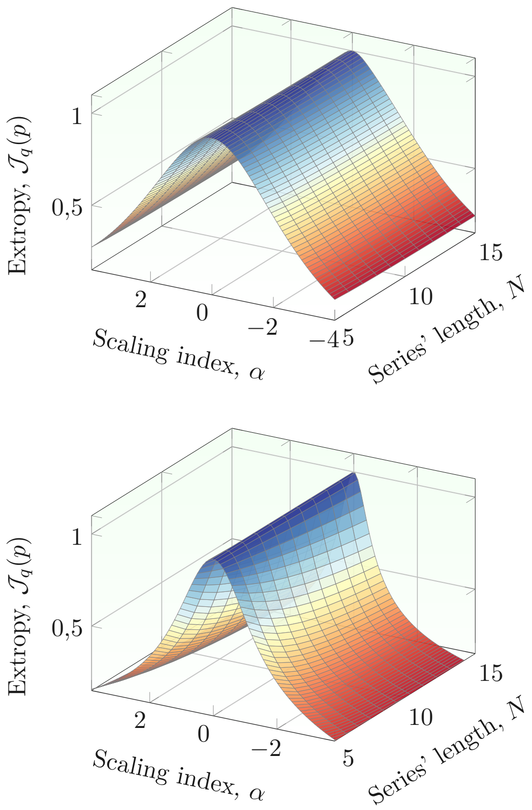

Figure 1: Wavelet Tsallis q-extropy of fractal signals. Top plot represents wavelet extropy (Tsallis extropy when $q \to 1$) and bottom plot wavelet Tsallis q-extropy with $q = 15$. Both information planes are computed with $\alpha \in (-4, 4)$ and $N \in (5, 15)$ to account for the effect of length in a range of the fractality exponent.

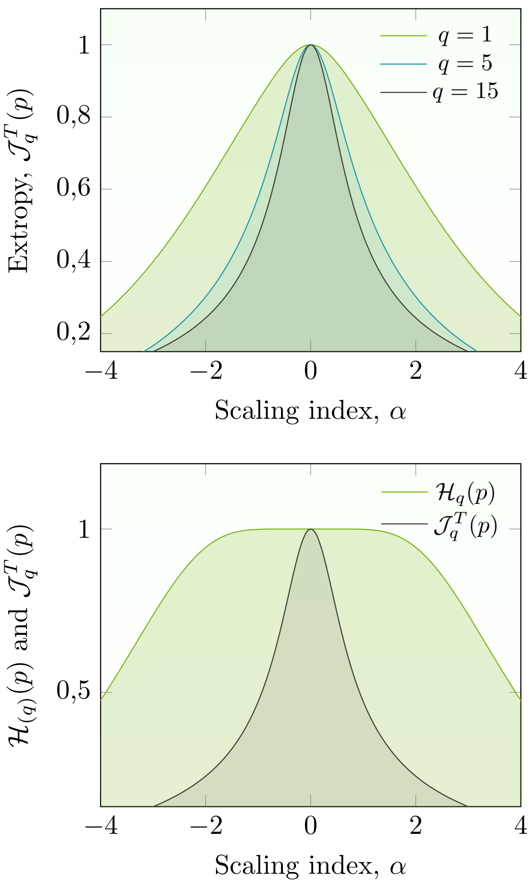

Figure 2: Wavelet tsallis q-extropy. Top plot shows the effect of the nonextensivity parameter q on the shape and characteristics of Tsallis extropies. Bottom plot shows a 2D comparison of Tsallis q-extropies and Tsallis q-entropies for the case $q = 15$.

Definition 1 *A q-extropy plane $\mathcal{E}^q$ is defined as a 3D surface plot of extropy values (computed using Tsallis or Rényi functionals) versus fractality parameter α and signal length N.*

Tsallis- q-extropy planes allow the characterization of the complexities of fractal signals and unveil potential applications. Fig. 1 shows the wavelet Tsallis q-extropy planes of fractal signals within the fractality range $\alpha \in (-4, 4)$ and signal lengths ranging from $N = 2^5$ to $N = 2^{15}$.

Top plot corresponds to the case $q = 1$, which represents wavelet Shannon extropy, while the bottom plot is the wavelet Tsallis extropy for the nonextensivity parameter set to $q = 15$. From Fig. 1, it is observed that for completely random fractals ($\alpha = 0$), extropies are maximum, increasing when $\alpha < 0$ and decreasing when $\alpha > 0$. In addition, for small q,

$$\mathcal{J}(p) > \mathcal{J}_q^T(p) \;\; \forall \alpha \in \mathbb{R}, \tag{15}$$

and as observed from the figure, signal length N has little or no effect on extropies values. Fig. 2 further studies the effect of nonextensivity parameter q on the form of extropies of fractal signals.

Top plot displays Tsallis extropies for various q and it is easily observed that for various q_j (q_j small), the following is satisfied,

$$\mathcal{J}_{q_1}^T(p) > \mathcal{J}_{q_2}^T(p), \;\; \forall \alpha \in \mathbb{R}, \tag{16}$$

as long as $q_1 < q_2$. This means that for increasing q,

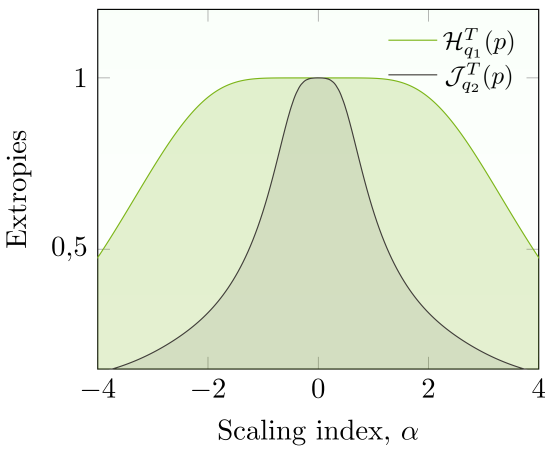

Figure 3: Wavelet Tsallis q-entropy $\mathcal{H}^T_{q_1}(p)$ ($q_1 = 15$) and Wavelet Tsallis q-extropy $\mathcal{J}^T_{q_2}(p)$ ($q_2 = 100$) plots within the fractality range $\alpha \in (-4, 4)$ and signal length $N = 2^{10}$.

Tsallis q-extropies are narrower up to point q_I, at which point extropies begin to be wider. However, as noted in this plot, when $q \geq 5$ this narrowness is not significant. Bottom plot of Fig. 2 shows a comparison of Tsallis q-extropy and Tsallis q-entropy for $q = 15$. From this plot, it is observed that,

$$\mathcal{J}^T_q(p) < \mathcal{H}^T_q(p) \quad \forall \alpha \in \mathbb{R}, \tag{17}$$

which means that Tsallis entropy is greater than Tsallis extropy in all the fractality range for all q. Fig. 3 shows a complementary comparison of Tsallis entropy and extropy when constant behaviour of entropies/extropies are observed. Tsallis entropies are obtained for $q_1 = 15$ and Tsallis extropies for $q_2 = 100$.

The constant extropy/entropy values are symmetrical to $\alpha = 0$ and these behaviours can be used for the classification of fractal signals. This constant range permits some fractal signals to be considered as white noise, while signals lying outside this range are considered correlated or noncorrelated fractals. By increasing the non-extensivity parameter in Tsallis extropies a wider constant region is observed and a different classification of fractal families may be achieved. Rényi extropies on the other hand, are obtained by direct application of

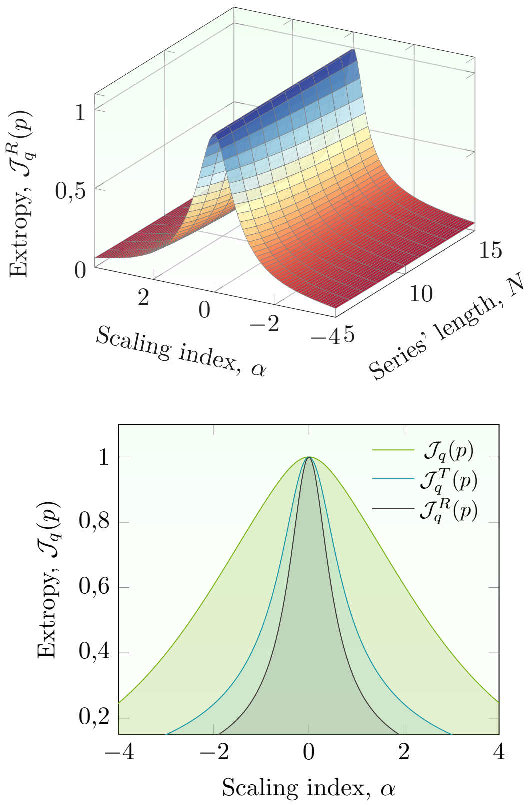

Figure 4: Wavelet Rényi q-extropy plane (top plot) for $q = 15$ in the fractality range $\alpha \in (-4, 4)$ and varying length. Bottom plot displays Wavelet extropies compared: wavelet extropy $\mathcal{J}(p)$, wavelet Tsallis q-extropy $\mathcal{J}^T_q(p)(q = 15)$ and wavelet Rényi q-entropy $\mathcal{J}^R_q(p)$ ($q = 15$).

Eq. (6) into Eq. (11), which results in

$$\mathcal{J}^R_q(p) = \Bigg\{ (N-1)\log\left(\sum_{k=0}^{q}\left(\frac{1-2^{\alpha N k}}{1-2^{\alpha k}}\right) \times \left(\frac{2^\alpha - 1}{1-2^{\alpha N}}\right)^k \binom{q}{k}\right) - (N-1) \times \log(N-1)\Bigg\} \times \frac{1}{1-q}. \tag{18}$$

Eq. (18) represents the wavelet Rényi extropy for fractal signals of parameter α.

Fig. 4 shows the Rényi information plane (top plot) for fractal signals in the scaling range $\alpha \in (-4, 4)$ and signal length from 2^5 to 2^{15}. Note from this plot that Rényi extropies are maximum for $\alpha = 0$ (white noise),

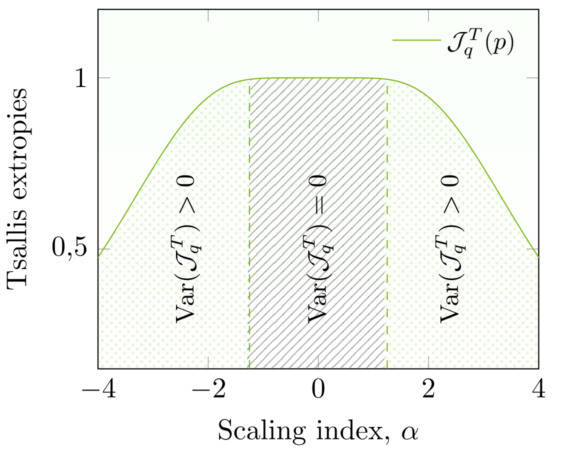

Figure 5: Heuristic for the classification of fractal signals with wavelet Tsallis q-extropies. Classification is perfomed based on constant/variable regions. If the process' variance is small, then it is considered a fractal belonging to the constant region, but if the variance is higher than some threshold, then it is considered a fractal belonging to the outside region.

increasing for noncorrelated fractals ($\alpha < 0$) and decreasing for correlated ones ($\alpha > 0$). In addition, Rényi extropies for fractals signals are independent of signal length N. Bottom plot of Figure 4 shows a comparison of wavelet extropy, Tsallis q-extropy and Rényi q-extropy (with identical q for q-extropies). From this plot it is easily observed that,

$$\mathcal{J}(p) > \mathcal{J}_q^T(p) > \mathcal{J}_q^R(p). \tag{19}$$

In addition,

$$\mathcal{J}_{q_1}^R(p) > \mathcal{J}_{q_2}^R(p), \quad \forall \alpha \in \mathbb{R} \tag{20}$$

for all $q_1 < q_2$. In constrast to wavelet Tsallis q-extropies, wavelet Rényi q-extropies do not have a constant region of extropies in some fractality range for a given q. This result is similar to those observed for standard wavelet q-entropies where the only entropy with constant regions is the wavelet Tsallis entropy. Accordingly, few applications of wavelet Rényi q-extropies can be mapped to fractal signals; however, it is a good descriptor of the complexities associated with fractal signals.

i Classification of fractals

As stated above, an example application of Tsallis q-extropies is in the classification of fractals. For this, Tsallis q-extropies must display a constant region. This constant region is observed on $|\alpha| < \alpha_C$ and therefore fractals within this interval experience small extropy variance while fractals whose fractality parameter is outside this interval experience longer variance. A simple heuristic for classifying fractals is therefore based on the observed variance of extropy values, small or no variance indicating a fractal signal lying in the class of fractals with parameter $|\alpha| < \alpha_C$ and extropies with significant variance indicating pertinence to the class of fractals outside $|\alpha| < \alpha_C$. Fig. 5 shows this heuristic based on the behaviour of extropies within the constant and nonconstant region in the wavelet Tsallis extropy plane. An interesting question is that which regards the length of the constant region for a specific q, or, equivalently, if q has some specific value, regarding which type of fractal can be discerned. Fig. 6 displays the relationship between extropic index q and upper-bound of constant region $|\alpha| < \alpha_C$. For instance, if $q = 150$ then it can classify fractals lying in the interval $|\alpha| < 0.4$, and when $q = 250$ a classification of processes in $|\alpha| < 0.5$ may be achieved. An additional level of classification may be obtained if the RWE is computed in another way.

ii Application to EEG signals

Wavelet Tsallis q-extropy can be employed for the analysis of complex fractal time series. In the following, EEG times series from [40] are briefly analyzed. The data consists of 100 surface EEG signals from healthy

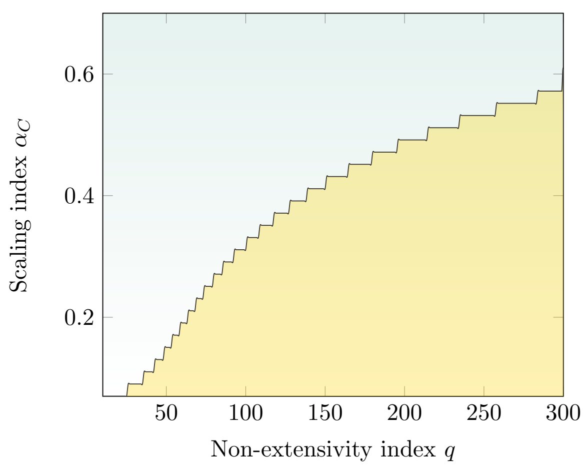

Figure 6: Relationship between extropic index q and upper bound of constant interval $|\alpha| < \alpha_C$

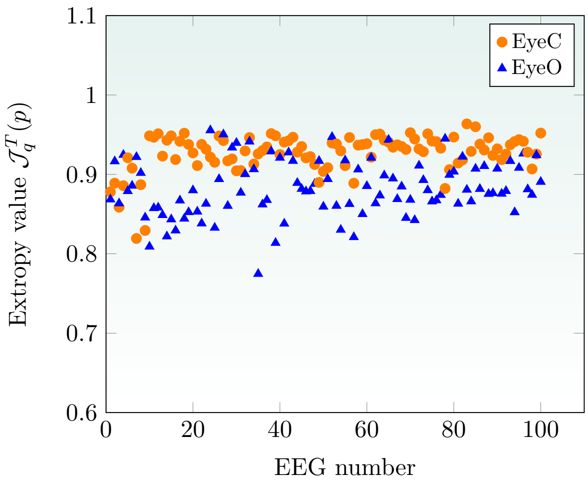

Figure 7: Wavelet Tsallis q-extropy calculation from surface EEG data with eyes open and eyes closed.

volunteers with eyes open and 100 with eyes closed. The experiment consists in only computing Tsallis q-extropy ($q = 300$) to every signal and then plotting the results. Fig. 7 shows the results, and, as can be observed at first glance, EEG time series from volunteers with eyes closed experience a higher Tsallis extropy value than those EEG time series from volunteers with eyes open. This means that the fractality parameter is near $\alpha = 0.5$, meaning the process is less correlated. Volunteers with eyes open therefore have a higher fractality parameter.

IV Conclusions

In this article, wavelet q-extropies of fractal signals were obtained by computing standard q-extropies on a time-scale representation of fractals. Closed-form expressions of wavelet Tsallis q-extropies and wavelet Rényi q-extropies were obtained and, based on these, extropy planes were computed. Extropy information planes allowed not only examination of the properties of these extropies, but also enabled the study of their relationships and, specifically, the relationship with standard wavelet q-entropies. Moreover, these planes allowed the highlighting of an example application of wavelet Tsallis q-extropies, specifically in the classification of fractal signals. Finally, the paper presented a simple application of wavelet Tsallis q-extropies for analysing EEG data.

Acknowledgements - Julio César Ramírez Pacheco is grateful for the support from the Cancún Multidisciplinary Division of the autonomous university of Quintana Roo. Authors also express thanks for the support from ITESO and CONAHCYT - Centro de investigación en matemáticas.

[1] A. Capurro, et al., *Tsallis entropy and cortical dynamics: the analysis of EEG signals*, Physica A, **257**, 149, (1998).

[2] W.-X. Ren and Z.-S. Sun, *Structural damage identification by using wavelet entropy*, Engineering Structures, **30**, 2840, (2008).

[3] O. Rosso, M. Martin, and A. Plastino, *Brain electrical activity analysis using wavelet-based informational tools (II): Tsallis non-extensivity and complexity measures*, Physica A: Statistical Mechanics and its Applications, **320**, 497, (2003).

[4] O. Rosso and A. Figliola, *Order/disorder in brain electrical activity*, Revista mexicana de física, **50**, 149, (2004).

[5] O. A. Rosso, et al., *Wavelet entropy: a new tool for analysis of short duration brain electrical signals*, Journal of neuroscience methods, **105**, 65, (2001).

[6] L. Zunino, et al., *Wavelet entropy of stochastic processes*, Physica A: Statistical Mechanics and its Applications, **379**, 503, (2007).

[7] Rosso, O. A., Martin, M. T., Figliola, A., Keller, K., & Plastino, A., *Wavelet entropy of stochastic processes*, Journal of neuroscience methods, **153**, 163-182, (2006).

[8] J. Ramirez-Pacheco, et al., *A nonextensive wavelet (q, q')-entropy for* $1/f^{\alpha}$ *signals*, Revista mexicana de física, **62**, 229, (2016).

[9] J. Ramírez-Pacheco, et al., *Wavelet Fisher's information measure of* $1/f^{\alpha}$ *signals*, Entropy, **13**, 1648, (2011).

[10] J. Ramírez-Pacheco, et al., *Wavelet q-Fisher information for scaling signal analysis*, Entropy, **14**, 1478, (2012).

[11] Pérez, D. G., Zunino, L., Martin, M. T., Garavaglia, M., Plastino, A., & Rosso, O. A., *Model-free stochastic processes studied with q-wavelet-based informational tools*, Physics Letters A, **364**, 259-266, (2007).

[12] J. C. Ramírez-Pacheco, et al., *Classification of fractal signals using two-parameter non-extensive wavelet entropy*, Entropy, **19**, 224, (2017).

[13] J. C. Ramírez-Pacheco, L. Rizo-Domínguez, and J. Cortez-González, *Wavelet-Tsallis entropy detection and location of mean level-shifts in long-memory fGn signals*, Entropy, **17**, 7979, (2015).

[14] L. Mastroeni, A. Mazzoccoli, G. Quaresima and P. Vellucci, *Wavelet analysis and energy-based measures for oil-food price relationship as a footprint of financialisation effect*, Resources Policy, **77**, 102692, (2022).

[15] O.A. Rosso, F. Olivares and A. Plastino, *Noise versus chaos in a causal Fisher-Shannon plane*, Papers in Physics, **7**, 070004, (2015).

[16] J.C. Piqueira, *A comparison of LMC and SDL complexity measures on binomial distributions*, Physica A: Statistical Mechanics and its Applications, **444**, 271-275, (2016).

[17] Huang, Y., Xiao, F., Cao, Z., & Lin, C. T. (2023). *Fractal Belief Rényi divergence with its applications in pattern classification*, IEEE Transactions on Knowledge and Data Engineering, **36**, 8297-8132, (2023).

[18] Huang, Y., Xiao, F., Cao, Z., & Lin, C. T. (2023). *Higher order fractal belief Rényi divergence with its applications in pattern classification*, IEEE Transactions on Knowledge and Data Engineering, **45**, 14709-14726, (2023).

[19] Xiao, F. (2023). *Quantum X-entropy in generalized quantum evidence theory*, Information Sciences, **643**, 119177, (2023).

[20] F. Lad, G. Sanfilippo, and G. Agro, *Extropy: Complementary dual of entropy*, Statistical Science, **30**, 40, (2015).

[21] Y. Xue and Y. Deng, *Tsallis extropy*, Communications in Statistics-Theory and Methods, **52**, 751-762, (2023).

[22] J. Liu and F. Xiao, *Renyi extropy*, Communications in Statistics-Theory and Methods, **50**, 1-12, (2021).

[23] J. Liu and F. Xiao, *Gini extropy*, Communications in Statistics-Simulation and Computation, **51**, 1-16, (2022).

[24] J. Murguia and E. Campos-Cantón, *Wavelet analysis of chaotic time series*, Revista mexicana de física, **52**, 155, (2006).

[25] M. Greiner, et al., *Wavelets: from signal analysis to the analysis of complex processes*, Revista Mexicana de Fisica, **44**, 11, (1998).

[26] J. P. L. Escola, et al., *The Haar wavelet transform in IoT digital audio signal processing*, Circuits, Systems, and Signal Processing, **41**, 4174, (2022).

[27] S. Stoev, et al., *On the wavelet spectrum diagnostic for Hurst parameter estimation in the analysis of Internet traffic*, Computer Networks, **48**, 423, (2005).

[28] D. Veitch and P. Abry, *A wavelet-based joint estimator of the parameters of long-range dependence*, IEEE Transactions on Information Theory, **45**, 878, (1999).

[29] P. Abry and D. Veitch, *Wavelet analysis of long-range-dependent traffic*, IEEE transactions on information theory, **44**, 2, (1998).

[30] A. López-Lambraño, et al., *Una revisión de los métodos para estimar el exponente de Hurst y la dimensión fractal en series de precipitación y temperatura*, Revista mexicana de física, **63**, 244, (2017).

[31] M. S. Taqqu, V. Teverovsky, and W. Willinger, *Estimators for long-range dependence: an empirical study*, Fractals, **3**, 785, (1995).

[32] G. Chan, P. Hall, and D. S. Poskitt, *Periodogram-based estimators of fractal properties*, The Annals of Statistics, **23**, 1684, (1995).

[33] Q. Zhou and Y. Deng, *Belief eXtropy: Measure uncertainty from negation*, Communications in Statistics-Theory and Methods, **50**, 1, (2021).

[34] N. Balakrishnan, F. Buono, and M. Longobardi, *On Tsallis extropy with an application to pattern recognition*, Statistics & Probability Letters, **180**, 109241, (2022).

[35] A. Noughabi and J. Jarrahiferiz, *On the estimation of extropy*, Journal of Nonparametric Statistics, **31**, 88-99, (2019).

[36] C.-K. Peng, et al., *Mosaic organization of DNA nucleotides*, Physical review e, **49**, 1685, (1994).

[37] J. R. Pacheco, D. T. Román, and H. T. Cruz, *Distinguishing Stationary/Nonstationary Scaling Processes Using Wavelet Tsallis q-Entropies*, Mathematical Problems in Engineering, **2012**, 916295, (2012).

[38] J. Ramírez-Pacheco and D. Torres-Román, *Cosh window behaviour of wavelet Tsallis q-entropies in $1/f^{\alpha}$ signals*, Electronics Letters, **47**, 186, (2011).

[39] J. Liu and F. Xiao, *On the maximum extropy negation of a probability distribution*, Communications in Statistics-Simulation and Computation, **50**, 1, (2021).

[40] Andrzejak RG, Lehnertz K, Rieke C, Mormann F, David P, Elger CE, *Indications of nonlinear deterministic and finite dimensional structures in time series of brain electrical activity: Dependence on recording region and brain state*, Phys. Rev. E, **64**, 061907, (2001).